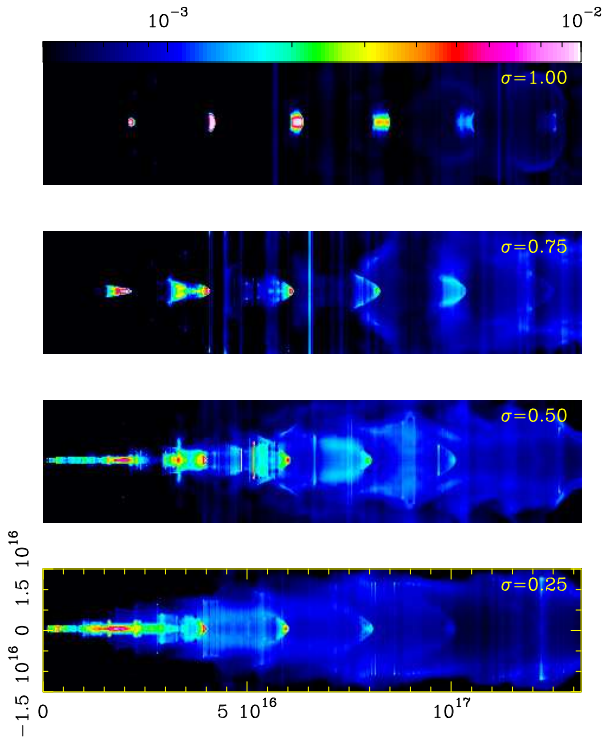

Fig. 3. [S II] 6716+30 intensity maps predicted from the four single-mode jet models with $n_a = 15$ cm^{-3} (see § 3) for a $t = 350$ yr integration time. The maps have been computed assuming that the outflow axis lies on the plane of the sky. Only a region close to the jet source is shown (compare with the full computational domain shown in Figures 1 and 2). The intensities are shown with a logarithmic color scheme given (in erg s^{-1} cm^{-2} sterad^{-1}) by the top bar. The color figure can be viewed online.

the knots with $x > 10^{17}$ cm. For lower values of σ, the emission knots have bow-wings of increasing intensity. The emission from these bow-wings partially fills in the gaps corresponding to the inter-knot regions (these gaps are clearly seen in the $\sigma = 1$ model, see Figure 3).

With these models we therefore show that the edge-to-center ejection velocity ratio σ has a strong effect on the morphology of the IWS (which results from the ejection velocity time-variability). For $\sigma = 1$ (i.e., for a top-hat jet, see equation 1), the [S II] emission of the IWS has a morphology of compact clumps, with low-emission gaps between the clumps. For lower values of σ, the emission from the IWS develops progressively more extended bow wings, which partially fill in the gaps between the successive knots. Therefore, by tuning the value of σ it is possible to produce knots with different morphologies, which could then be compared with the emission observed in specific HH jets. An attempt to do this is presented in the following section.

4. THREE-MODE MODEL FOR HH 34

Raga & Noriega-Crespo (1998) and Raga et al. (2002) proposed a three-mode ejection velocity variability for modelling the structure of the southern lobe of the HH 34 outflow. In particular, Raga et al. (2002) used radial velocity and proper motion observations of HH 34 to derive a variability of the form:

$$v_c(t) = v_0 + v_1 \sin\left(\frac{2\pi t}{\tau_1} + \phi_1\right) + v_2 \sin\left(\frac{2\pi t}{\tau_2} + \phi_2\right) + v_3 \sin\left(\frac{2\pi t}{\tau_3}\right), \quad (2)$$

with $v_0 = 270$ km s^{-1}, $v_1 = 70$ km s^{-1}, $\tau_1 = 1400$ yr, $\phi_1 = -0.80$ rad, $v_2 = 25$ km s^{-1}, $\tau_2 = 270$ yr, $\phi_2 = -0.85$ rad, $v_3 = 10$ km s^{-1} and $\tau_3 = 27$ yr. This function represents the past time-variability of the ejection of HH 34, with $t = 0$ representing the present time. Negative values of t represent the times at which the material presently observed along the HH 34 jet was ejected from the source.

We then choose an ejection velocity v_j with this three-mode variability, modulated with a quadratic center-to-edge profile:

$$v_j(r,t) = v_c(t)\left[1 - (1-\sigma)\left(\frac{r}{r_j}\right)^2\right], \quad (3)$$

where $v_c(t)$ is given by equation (2) and σ is the center-to-edge ejection velocity ratio (see equation 1).

Following Raga et al. (2002), we choose time-independent, top-hat ejection density and temperature cross sections with $n_j = 5000$ cm^{-3} and $T_j = 1000$ K (respectively), and a $r_j = 5 \times 10^{15}$ cm jet radius. The jet moves into a homogeneous environment with $n_a = 15$ cm^{-3} and $T_a = 1000$ K.

The computational domain has an (axial $\times$ radial) extent of $(16.8, 2.1) \times 10^{17}$ cm, resolved with 4096×512 grid points at the highest resolution of the 6-level, binary adaptive grid. The setup of the three-mode models is otherwise identical to the one of the single-mode models described in § 3.

We have then computed three models, with center-to-edge ejection velocity cross sections with $\sigma = 1$, 0.75 and 0.5. The simulations were all started at $t = -3000$ yr, and allowed to evolve until $t = 300$ yr.